



HAL
open science

A Novel Thermoplastic Composite for Marine Applications: Comparison of the Effects of Aging on Mechanical Properties and Diffusion Mechanisms

Haithem Bel Haj Frej, Romain Léger, Perrin Didier, Patrick Ienny

► To cite this version:

Haithem Bel Haj Frej, Romain Léger, Perrin Didier, Patrick Ienny. A Novel Thermoplastic Composite for Marine Applications: Comparison of the Effects of Aging on Mechanical Properties and Diffusion Mechanisms. *Applied Composite Materials*, 2021, 28, pp.899-922. 10.1007/s10443-021-09903-0 . hal-03201968

HAL Id: hal-03201968

<https://imt-mines-ales.hal.science/hal-03201968>

Submitted on 25 May 2021

HAL is a multi-disciplinary open access archive for the deposit and dissemination of scientific research documents, whether they are published or not. The documents may come from teaching and research institutions in France or abroad, or from public or private research centers.

L'archive ouverte pluridisciplinaire **HAL**, est destinée au dépôt et à la diffusion de documents scientifiques de niveau recherche, publiés ou non, émanant des établissements d'enseignement et de recherche français ou étrangers, des laboratoires publics ou privés.

A novel thermoplastic composite for marine applications: Comparison of the effects of aging on mechanical properties and diffusion mechanisms

Haithem Bel Haj Frej^{1}, Romain Léger¹, Didier Perrin², Patrick Lenny¹*

¹ *LMGC, IMT Mines Ales, Univ Montpellier, CNRS, Ales, France*

² *Polymers Composites and Hybrids (PCH), IMT Mines Ales, Ales, France*

**Corresponding author: haithem.bel-haj-frej@mines-ales.fr*

Abstract

This article investigates and compares the effects of hydrothermal aging on carbon fibre / Elium™ thermoplastic composite and on carbon fibre / vinylester thermoset composite for marine application. Accelerated aging tests are performed by immersion in deionised water at 70 °C. Water diffusion, monitored by regular weighing, shows that both composites as well as Elium™ resin exhibit non-Fickian behaviour. Analytical models are proposed to fit the experimental curves and to identify and compare diffusion parameters. The aging effects on the microstructure are evaluated using SEM, while irreversibility of degradation mechanisms is investigated by desiccation tests. Mechanical tensile tests, performed before and after aging, show the slight impact of water on tensile modulus and tensile strengths for both materials. Furthermore, it was found that shear modulus and interlaminar shear strength undergo significant alteration related to irreversible physicochemical degradation of the matrix. Studied materials have shown different diffusion behaviours, but similar mechanical properties evolutions.

Keywords

Durability; Thermoplastic resin; Thermosetting resin; Mechanical testing

1. Introduction

During last few decades, composite materials have replaced wood and metals in many marine applications such as sailing and pleasure boats. The first composite boats appeared in the early 60s, nowadays, more than 90% of pleasure boats are made from composites. While thermoset composites are generally used in producing large marine structures by resin infusion process, their thermoplastic counterparts are less present in marine applications due to specific parts processing methods like autoclave and compression moulding. Thermoplastic composites offer considerable advantages such as increased toughness, recyclability and reparability. Recently, a new thermoplastic acrylic resin, called Elium™, has been developed by Arkema [1]. The Elium™ 188-O resin have the advantage of being liquid and having a low-viscosity (≈ 100 mPa.s) at 25 °C [2]. This novel reactively polymerized liquid thermoplastic resin opens new possibilities for room temperature manufacturing processes such as Vacuum Assisted Resin Infusion (VARI) [3,4] and Vacuum Assisted Resin Transfer Moulding (VARTM) [5–7]. The acrylic resin undergoes radical polymerization by peroxide compounds initiation resulting in a PMMA like matrix [8]. During the curing step, covalent bonds are created to obtain entangled macromolecular chains with strong interactions between methacrylate side groups and primary carbon of the main chain. In return, thermosets are cross-linked polymers with a single three-dimensional macromolecular chain. Several authors have compared mechanical properties like tensile, compressive, shear and impact performances of Elium™ based composites to their thermoset-reinforced counterparts. Results are found to be in the same range, except for impact resistance as acrylic composites show significant higher results [9–11].

Over their service life in marine environment, boats are subjected to various and coupled stresses. In addition, the temperature, composition and salinity of seawater are known to be harmful for materials when exposed for long periods [12]. Despite the layers of protection applied to the structure, the harsh environment may cause harmful damages to the submerged parts. The aging of composites in immersion can be described by several phenomena like diffusion in which water

molecules ingress into free volumes of the material [13]. Other marine aging effects on composites can be osmosis, blistering, marine fouling, cavitation and erosion. The consequence of composite aging under moisture and/or water are either physical or chemical [12,14]. Physical aging includes reversible phenomena such as plasticization and swelling, which are characterised by the alteration of the spatial configuration of polymer macromolecular chains without any modification of their chemical structure. On the other hand, chemical aging concerns any phenomena involving a chemical modification of the material like hydrolysis. Both of those two aging mechanisms are usually superimposed. At macroscopic scale, the kinetics of water diffusion into composite material are frequently modelled by Fick's second law as presented in the theoretical development of Crank [15]. The water content rises gradually and then reaches a saturation plateau depending on the polarity [16] and the solubility parameters of the polymer [12]. The saturation water content is an indicator of the hydrophilic affinity of polymer matrices. When exposed to moisture, the liquids penetration tends to spread polymer macromolecules inducing an increase of the mobility of molecular chains and shorter molecular side-groups having an increase in the free volume of the polymer as a consequence. These phenomena generally lead to a lowering of polymer's glass transition temperature. When such phenomena occur in polymers, or when the composite presents structural defaults, a deviation from Fickian diffusion is generally reported and thus semi-empirical Fickian-modified models are developed to assess diffusion kinetics. If the matrix itself exhibits abnormal behaviour also called non-Fickian behaviour, then the entire composite will have non-Fickian behaviour. Then again, if the composite contains porosities, cracks or delamination, the diffusion can be altered. Several authors have developed different models in order to better understand the material "anomalous" response. Bao and Yee [17,18] and Roy et al.[19] proposed a time-dependent diffusion coefficient model in order to fit their experimental results. Chen et al. [20] proposed a concentration-dependent diffusion coefficient model, while Weitsman [21] proposed a time dependant boundary condition. Other authors were interested in Fickian models where diffusion-relaxation coupling is taken into account suggesting that an initial part of the absorption is dominated by diffusion,

while the second stage is dominated by relaxation. In other words, moisture transport is a combined effect of physical diffusion and chemical interactions. Carter and Kibler developed a Langmuir based model, which supposes that a part of the solvent molecules diffuses freely in the accessible free volume, while the other part is retained by weak interactions with hydrophilic sites [22]. More complex models were developed on the basis of chemical degradation occurring simultaneously with diffusion [23], and on diffusion in cavities [24].

In terms of water diffusivity and marine durability, few works were already published concerning Elium™ and Elium™ based composites, compared to deeply studied thermoset based counterparts [25]. Immersion effects of neat Elium™ resin and its glass or carbon fibre reinforced composites in seawater are found to be recoverable after drying. Compared to a marine grade epoxy resin system, the durability is found to be slightly better. In higher aging temperatures, irreversibility of the drop in mechanical properties is related to poor fibre/matrix adhesion due to incompatible sizing [26]. Despite the fact that Elium™ resin showed Fickian behaviour at different aging temperatures, non-Fickian behaviour is observed for carbon and glass fibre/Elium™ composites [27]. Aging effects on fatigue behaviour of acrylic matrix composites under tensile and flexural loading showed good recovery of properties compared to glass and carbon reinforced marine grade epoxy [28].

In this work, hydrothermal aging behaviour of the Elium™ neat resin and carbon fibre reinforced acrylic resin are investigated at a constant temperature in analogy with an equivalent thermoset composite usually used in marine applications. Diffusion parameters based on both Fickian and modified-Fickian models are compared using optimisation algorithm in order to better understand degradation phenomenology. Based on both microscopic observations and quasi-static mechanical properties, the changes in microstructure and the effects of aging are discussed.

2. Materials & methods

2.1. Materials and manufacturing process

In this study, a commercial balanced carbon fibre stitched biaxial fabric is used. It is a Cbx600 24K T620 from Sicomin with a density of 1.77 g/cm³ and areal weight of approximately 629 g/m². It consists of two UD layers (T620SC-24k-50C 1850 tex) of an areal weight of 309 g/m², each superposed in $\pm 45^\circ$ directions and stitched by a thermoplastic polyester (PES) binding yarn of an areal weight of 9 g/m². The compatibility of the fabric is for general use like epoxy, polyester, vinylester, and phenolic resin. No special sizing for acrylic resin is used. Two resins are used in this study; the first is the Elium™ 188-O kindly provided by Arkema (Lacq, France). The detailed formulation given by the supplier shows that the majority of the polymer consists of a methyl methacrylate copolymer (70 – 90%), citral ($\leq 5\%$), hydro-treated light paraffinic distillates (petroleum) ($\leq 2\%$) and other additives. When the Perkadox CH-50X dibenzoyl peroxide initiator (AkzoNobel) is added to the liquid polymer, it undergoes radical polymerization followed by an exothermic peak. According to datasheet, recommended peroxide ratio is from 1.5% to 3% depending on the reactivity needed. The polymerization occurs at room temperature so no need for post-curing. However, Arkema recommend a post-curing at 80 °C for 4 hours for optimal mechanical properties [29]. The second resin is a pre-accelerated epoxy bisphenol-A vinylester modified resin Atlac® E-Nova MA 6215 from Aliancys. The low viscosity vinylester resin (80 – 90 mPa.s), hereinafter called ‘VE’, can be cured with normal methyl ethyl ketone peroxide like Butanox M50 and is formulated for marine applications. Table 1 compares the physical and mechanical properties of the two resin systems at 25 °C and 3% of Benzoyl peroxide (BPO) initiator CH50X and Butanox M50 hardener for Elium™ 188-O and VE resins, respectively.

Table 1 : Comparison of the physical and mechanical properties of Elium™ 188-O and VE resin

Properties	Elium™ 188-O	Vinylester
Viscosity (mPa.s)	100	80-90
Density (g/cm ³)	1.2	1.18
Peak time (minutes)	55	70 – 82
Heat Deflection Temperature (°C)	109	105
Tensile Strength (MPa)	76	70
Tensile Modulus (GPa)	3.3	4
Tensile Deformation (%)	6	2 -3
Flexural Strength (MPa)	130	120
Flexural Modulus (GPa)	3.25	4

To produce neat resin samples, casting method is used. Elium™ resin and BPO initiator were manually mixed in a weight ratio of 3%, and then the mixture was casted vertically between two rectangular glass plates covered with Teflon sheet to ensure demoulding. The same method was used for vinylester resin and M50 hardener mixture. The 4 mm thickness plates hereby casted were left to polymerize for 24 hours at room temperature in the closed mould. Composite plates of 400×400 mm² were manufactured by resin infusion at room temperature. Once the resin flow achieved the end of the 4 plies fabric stack, resin inlet and vacuum outlet are closed. The infused plate was left to polymerize at room temperature for 24 hours. As for neat resin samples, no post-curing of composite plates was performed because, in contrast with boat manufacturing process in the shipyard, infused boats are left to cure at ambient temperature.

Fibre, matrix, and void volume fractions calculations are performed using density measurements with helium gas pycnometer of composite samples cut at random emplacement of the plate. The fibre volume fraction V_f (%) is calculated using Equation 1 below.

$$V_f = \frac{W_f}{\rho_f \times V_c} \times 100 \quad \text{Equation 1}$$

Where ρ_f is the fibre density (g/m^3), V_c is the composite volume (m^3) and W_f is fibre weight (g), calculated using Equation 2.

$$W_f = A_w \times N \times L \times l \quad \text{Equation 2}$$

Here, A_w is the fabric areal weight (g.m^{-2}), N is the number of plies, L and l are the composite length (m) and width (m) respectively. Equation 3 gives the resin volume fraction V_r .

$$V_r = \frac{W_c - W_f}{\rho_r \times V_c} \times 100 \quad \text{Equation 3}$$

Where W_c is the composite weight (g) and ρ_r is the resin density (g/m^3). Finally, the void volume fraction V_p is calculated using Equation 4.

$$V_p = 100 - V_f - V_r \quad \text{Equation 4}$$

Once demoulded, the plates were stored in a climatic chamber at 23 °C and 50% RH until sample preparation. For that, a circular saw is used with water cooling system. Different samples dimensions were cut according to the tests requirements. The details about infused plates and different constituent fractions are presented in Table 2. The values given here are the average of at least two measurements with standard deviation in brackets.

Table 2: Processing parameters of infused composite plates

Material	CF/ Elium™ 188-O	CF/Vinylester
Laminate sequence	[(0/90) ₄]	[(0/90) ₄]
Fibre weight fraction	71.2 (0.28)	71.1 (1.13)
Fibre volume fraction	61.8 (1.94)	59.0 (0.65)
Resin volume fraction	33.8 (1.98)	38.7 (0.24)
Void volume fraction	4.5 (0.04)	2.2 (0.40)

2.2. Sample conditioning and accelerated hydrothermal aging

Before starting the accelerated aging test, samples were conditioned in a laboratory oven at 40 °C and less than 10% RH for nearly 40 days. The weight of the samples was monitored until reaching an effective equilibrium state. Then samples of both neat resins and carbon fibre reinforced

Elium™ (denoted CF / Elium™) and carbon fibre reinforced vinylester (denoted CF / VE) materials were immersed in deionised water which is shown to be more aggressive in terms of moisture absorption and the consequent decrease in material properties than seawater and salty water for polymers and their composites [30,31]. A high temperature of 70 °C was chosen to accelerate the diffusion process with respect to both Elium™ 188-O and VE resin glass transition temperature (T_g), which were found to be 102.5 °C and 115.7 °C, respectively, to avoid any activated side effects. Once immersed, samples weight is monitored using a ±0.1 mg accurate scale (Sartorius Secura225D-1S) according to ASTM D 5229/D 5229M – 92 standard specifications. The average amount of absorbed water in a sample M_t (%) was taken as the ratio of the mass of the water in the material to the mass of the oven-dry material and expressed as follows [32]:

$$M_t(\%) = \frac{W_i - W_0}{W_0} \times 100 \quad \text{Equation 5}$$

Where W_i is the current specimen mass and W_0 is the oven-dry specimen mass. The water uptake is measured regularly during aging and then water absorption is reported as a function of square root of time. Once a saturation plateau was achieved, some samples were tested to check the mechanical properties at the aged state. In addition, other samples were dried in the oven at 40 °C until reaching an equilibrium state. Figure 1 represents a detailed scheme of the implemented aging protocol. The purpose of this aging scheme is to assess the effect of different material state, depending on their water content, on the mechanical properties. The reversibility of the aging is also studied via the final drying step.

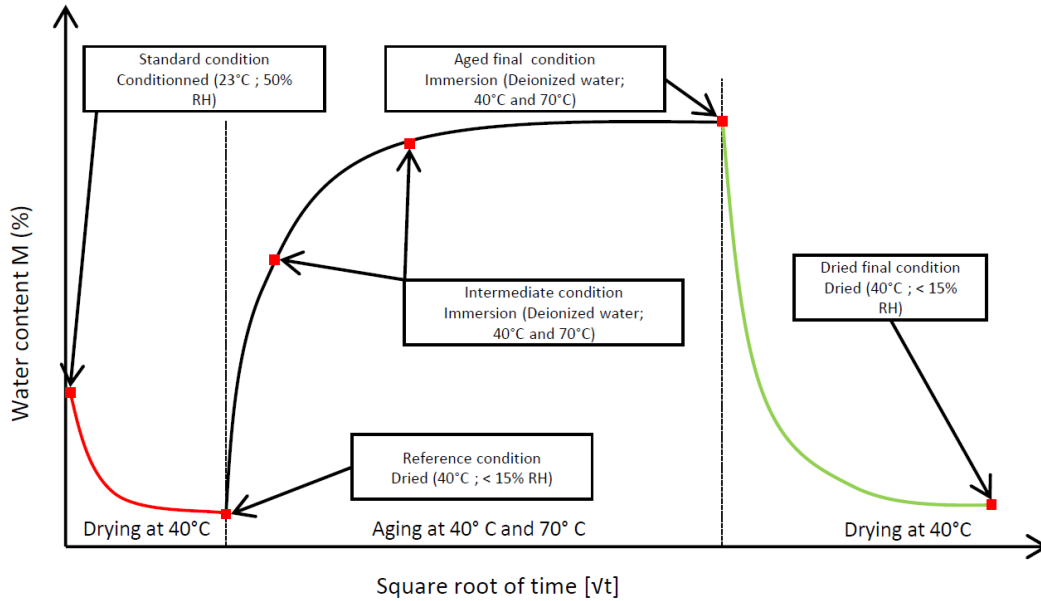


Figure 1 : Scheme of the aging methodology

2.3. Mechanical properties assessment

Quasi-static tensile test:

Tensile tests were performed accordingly to the ISO 527-4 standard on an MTS Criterion 50 tensile machine equipped with a 100 kN load cell. Sample dimensions are 250 mm length, 25 mm width and around 2.5 mm thickness. After surface sanding and cleaning, aluminium tabs (50×25×2 mm³) were bonded to the tests specimens using Loctite Super Glue 3 adhesive. Then, test specimens were painted and speckled in order to use digital image correlation (DIC) to evaluate the in-plane strain tensor [33]. All the tensile tests were carried out at a crosshead speed of 1 mm/min in ambient atmosphere. Samples were tested at the reference and the final aged condition (Figure 1). Images for DIC and load were simultaneously acquired by a LabVIEW software.

Interlaminar Shear strength analysis:

Commonly referred as ILSS, the short-beam test method was used to monitor the quality of fibre/resin bond in the interphase area by means of failure resistance calculations and failure modes observations. According to ASTM D2344 / D2344M standard, the test consists of a three-

point bending test with adapted close support on a Zwick-Roell testing machine (model B Z010/TH) (Figure 2)

For this test, specimens were machined from plates of 5 mm thickness (8 plies of carbon fibre fabrics). Samples were cut in accordance with the recommendations of the standard, with a span length of 20 mm and the dimensions were $(30 \times 10 \times 5) \text{ mm}^3$. The load was applied at 1 mm/minute on load cell of 10 kN and an accuracy of 0.1 N. The apparent interlaminar shear strength τ , expressed in MPa, is calculated using the following equation:

$$\tau = \frac{3}{4} \times \frac{P_m}{b \times h} \quad \text{Equation 6}$$

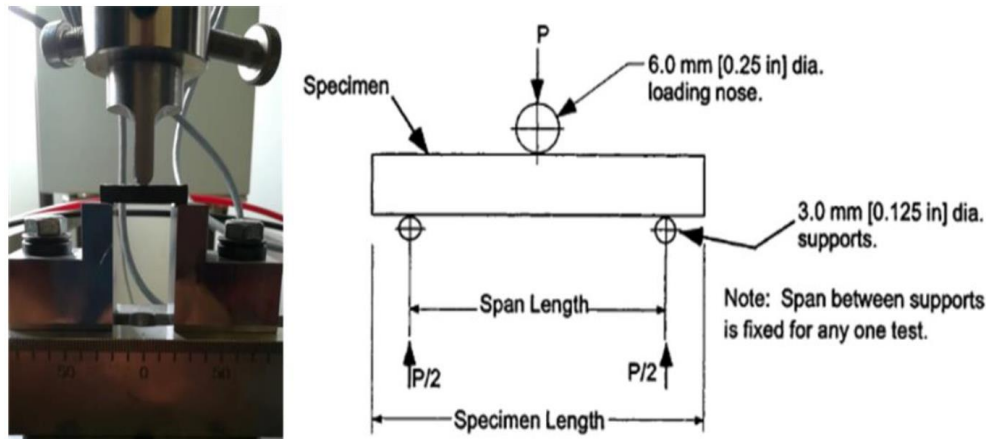


Figure 2 : ILSS device (left) and test diagram (right) for rectangular laminates

where: P_m is the maximum load observed during the test (N), b and h are the measured width and thickness (mm), respectively.

2.4. Scanning Electron Microscopy (SEM):

Scanning electron microscopy can provide more detailed information on the fibres, matrix and fibre/matrix interface state. All those components have been observed before and after aging. An FEI Quanta 200 FEG was used for image acquisition. To do so, polished sections were prepared by casting a polymer in a specimen holder. After polymerization, the top surface of the samples was polished and a thin carbon foil was applied using a Balzers CED030 metal coater.

3. Results and discussion

3.1. Kinetics of water absorption

3.1.1. Case of resins

In this study, hydrothermal aging mechanisms are accelerated by increasing the temperature. The experimental and numerical fitted water absorption curves as a function of the immersion time of both resin systems samples of identical dimensions are presented in Figure 3. For VE resin coupons (Figure 3.a), having dimensions of $50 \times 50 \times 4 \text{ mm}^3$, absorption curves follow a typically Fickian diffusion, explained by an almost unidirectional diffusion through the thickness of the plates, and can be divided into two stages. The first part shows a linear evolution of the quantity of water absorbed as a function of the square root of time. After 170 hours of immersion, an intermediate equilibrium plateau is observed at the level of 1.15% of the amount of water absorbed. Then, after about 1700 hours, a new build-up is observed. This phenomenology known as two-stage water diffusion is related to irreversible reactions between the polymer chains and water, with the formation of hydrogen bonds [34]. For Elium™ 188-O resin, the diffusive behaviour is different. A first linear part up to 64 hours of immersion and around 2% of water content is followed by a change of the slope. The behaviour is non-Fickian since a saturation plateau is not reached during the total immersion period. This type of diffusive behaviour shown in Figure 3.b is usually accompanied by a phenomenon of damage, which increases over time [35]. According to the manufacturer, the Elium™ resin consists of around 50% to 85% of methyl methacrylate (MMA) monomer. In the literature, the saturation level of Poly(methyl methacrylate) (PMMA) is about 2.2% at 27 °C [36]. In the presence of high temperature, the mechanism of aging is accelerated and the PMMA undergoes hydrolysis at the level of the lateral groups. Water molecules diffuse into the material by establishing hydrogen bonds with the polar carbonyl groups of PMMA. There is then a change in the polarity of side groups: more polar acid groups replace the initial groups. The formation of these acidic groups causes an increase in

hydrophilicity. It has been shown that in PMMA whose polarity has been increased, absorbed water forms clusters on the surface of the material [37].

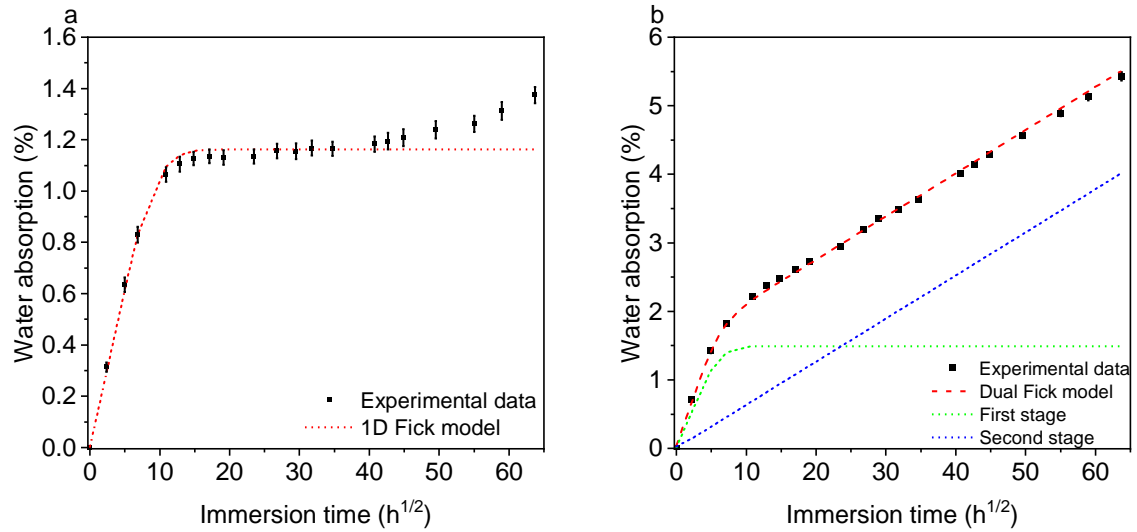


Figure 3 : Experimental data and model results of water absorption as a function of the square root of the immersion time of (a) VE and (b) Elium™ resin specimens immersed in water at 70

°C

3.1.2. Case of composites

Carbon fibre reinforced vinylester and Elium™ composite specimens are immersed in deionised water. At relatively high temperatures, sorption mechanisms are accelerated and degradations can worsen. For both composites, mass gain curves square shaped specimens ($180 \times 180 \times 2.5 \text{ mm}^3$) are shown hereafter. Figure 4.a shows the evolution of the amount of water absorbed for CF / VE composite samples. The first part of the curve is linear, which corresponds to Fickian diffusion kinetics. A pseudo-saturation plateau is then observed at the level of 0.35% of water content, before a gradual drop in the overall mass gain. This instability, due to the high temperature of aging, corresponds to a loss of weight related to an irreversible chemical degradation. The chemical decomposition occurs mainly in the form of decohesion between the fibres and the polymer, caused by leaching along the fibre / matrix interphase, as well as by hydrolysis, *i.e.* breaking of the lateral groups of polymer chains followed by chain splitting [35]. This phenomenon has been observed by Kootsookos et al. [38]. Considering that the crosslinking of

vinylester resins at room temperature is usually not complete without post-curing, the ester groups contained in the vinylester resin undergo hydrolysis, thus forming carboxylic acids and alcohols. The hydrolysis reaction promotes the extraction of the low molecular weight vinylester species, unreacted styrene and glycols from the composite into the water. Kootsookos et al. demonstrated this reaction by analysing seawater before, during and after immersion of the glass fibre / polyester composites [38]. Results of infrared spectroscopy show the presence of organic compounds that are not crosslinked. These are mainly chemical entities with hydroxyl end groups. In the case where the composites have undergone post-curing, the loss of mass is less pronounced compared to that of the non-post-crosslinked composites. This leaching-related loss of mass is systematic for polyester resin composites reinforced with glass or carbon fibres. This phenomenon has also been observed by several authors [30,39–41].

Mass gain curves of CF / Elium™ composite material during aging are shown in Figure 4.b. The evolution of the water content is not linear and a near-saturation plateau corresponding to 6.8% is reached after about 3400 hours of immersion. The amount of water absorbed is very important compared to CF / VE composites. This can be related to the already shown larger hydrophilicity of Elium™ resin, which when immersed at 70 °C, moisture uptake increases drastically without reaching saturation. This water ingress catalyses the hydrolysis of unreacted methyl methacrylate monomer. With respect to the composites, this chemical degradation causes a debonding of the fibres promoting the diffusion of water by capillary action along the fibre/matrix interface. It is also necessary to mention that significant changes in colour and transparency have been observed on Elium™ resin and CF / Elium™ composite test specimens.

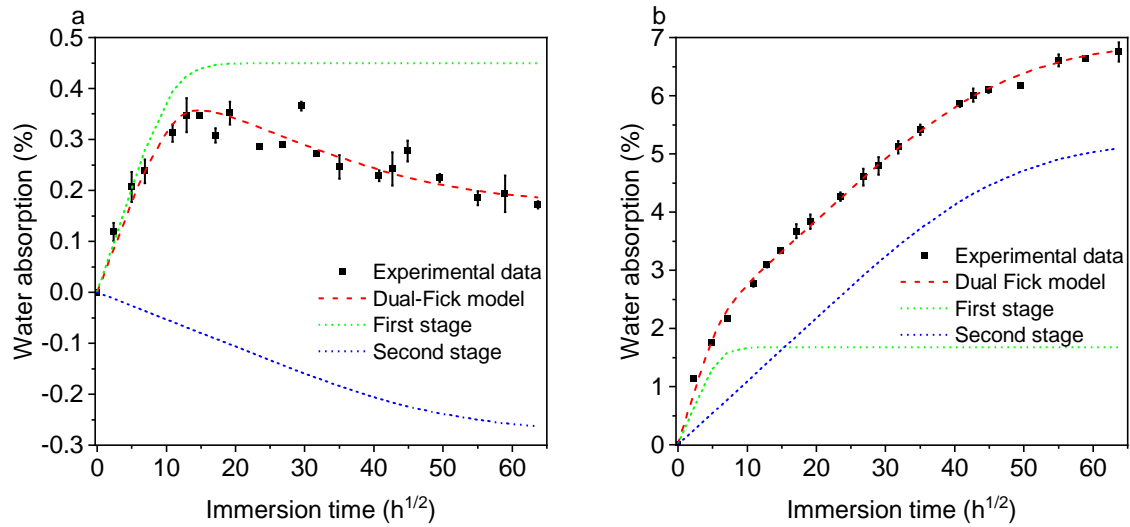


Figure 4 : Evolution of water absorption as function of the square root of the immersion time of
 (a) CF / VE and (b) CF / Elium™ composite specimens

SEM images presented in Figure 5 show microstructural defects of unaged CF / Elium™ composites at the interply area compared to CF/VE composite.

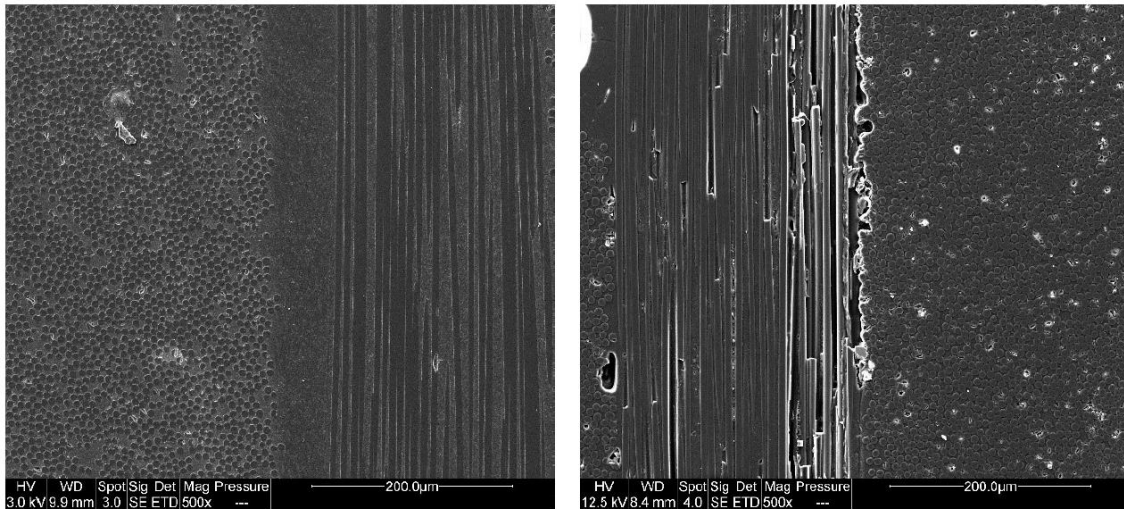


Figure 5 : SEM pictures of the microstructure of CF / VE (left) and CF / Elium™ composite
 (right) before aging

3.2. Reversible and irreversible changes induced by hydrothermal aging

In order to examine the reversibility of aging mechanisms, drying was performed in air circulating oven at 40 °C and weight loss curves are presented in Figure 6 for both CF / VE and CF / Elium™ tensile composite samples as well as neat resins samples. Both composites reached a stabilisation

after 96 hours of desiccation. For neat resins samples, mass variation is slower, and an equilibrium plateau is reached after about 900 hours, then no more mass loss is observed. At this stage the Elium™ resin samples have lost 0.31 % of their dry initial weight (before aging), and this constitutes around 5 % of the total water content at saturation stage. In return, VE resin samples have lost more than 0.34 % from their dry initial weight, but this represents around 30% of the total water content when the equilibrium plateau is established during aging test. This leads to suggest that, for VE resin, irreversible degradation took place during aging. This degradation can be attributed to the hydrolysis of vinylester matrix by water molecules, and also to leaching of non-cross-linked vinylester monomers as detailed in 3.3.2. Furthermore, composites reached a dried mass 1% and 0.6 % lower than initial state before immersion for CF / Elium™ and CF / VE composites, respectively. This residual weight loss of composite samples after desiccation could be explained by hydrolysis of the thermoplastic and thermosetting matrices when subjected to harsh aging conditions. This causes fibre/matrix interface weakening. In addition, leaching phenomenon could also lead to an increase in the void volume content and so a drop in mechanical properties. Several authors have reported the drop in mechanical properties (tensile strength, modulus, shear strength and modulus) because of accelerated aging tests. Silva et al reported a decrease of tensile strength when carbon fibre/epoxy and carbon fibre/vinylester rods were immersed in seawater [42]. In the same context, Arhant et al. [43] found that longitudinal strength and modulus of UD carbon fibre reinforced thermoplastic composites were not significantly affected by aging in sea water at 40 °C. For tensile tests in transverse direction and shear tests, a considerable decrease in mechanical properties is observed, especially when water content exceeded 1%. Thus, the noticeable drop in off-axis mechanical properties and interlaminar shear strength is directly related to irreversible degradation occurring during aging.

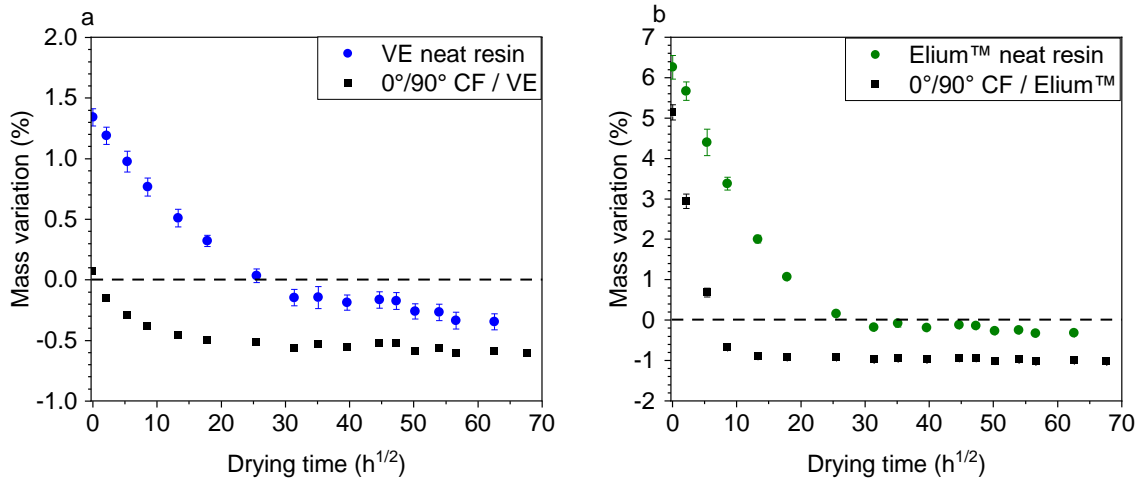


Figure 6 : Evolution of water content during drying test at 40 °C of Elium™ (a) and vinylester (b) neat resin and composite samples

3.3. Modelling of the diffusion

All organic resins absorb water to some extent, while glass and carbon fibres are considered inert. Several works studied the effects of long-term water absorption. Fick did the quantitative exploitation of the diffusion by adopting the mathematical equation of heat transfer developed by Fourier. According to Pritchard [44], a moisture absorption is of Fickian type if the absorption and desorption curves (gain and loss of weight) plotted as a function of square root of time are linear up to 60% of the maximum water content M_m . In this case, water absorption with constant diffusivity can be modelled by applying the second Fick diffusion law as a function of diffusion coefficient D expressed in $m^2.s^{-1}$ and the moisture concentration c .

$$\frac{\partial c}{\partial t} = \text{div}(-D \overrightarrow{\text{grad}} c) \quad \text{Equation 7}$$

In the case of a homogeneous material of infinite dimensions ($e \ll L$ and $e \ll l$), the one-dimensional Fick's second law can be written as:

$$\frac{\partial c}{\partial t} = D \frac{\partial^2 c}{\partial x^2} \quad \text{Equation 8}$$

Taking into account the initial and boundary conditions of the concentration and integrating the solution of Equation 8 over the thickness of the material, the following equation is obtained:

$$\frac{M_t}{M_\infty} = 1 - \frac{8}{\pi^2} \sum_{n=0}^{\infty} \frac{1}{(2n+1)^2} \exp\left(\frac{-\pi^2 D t (2n+1)^2}{e^2}\right) \quad \text{Equation 9}$$

Where M_t is the water content at time t expressed by Equation 5, M_∞ is the water content at equilibrium and e is the thickness. In order to identify unknown parameters of Equation 9, an optimisation approach relying on the construction of an objective function q is given by:

$$q = \sum_i [M_t(t_i) - M_i]^2 \quad \text{Equation 10}$$

With $M_t(t_i)$ is the water content calculated from Equation 9 at time t_i and M_i is the experimental water content extracted from the gravimetric curve. Minimizing the function q allows the identification of different unknowns by adjusting the diffusion curve according to Fick's law to the experimental data. The optimization algorithm is done with Matlab® software using a metaheuristic routine called PSO (Particle Swarm Optimization).

3.3.1. Case of resins

Samples of vinylester resin are immersed in deionised water at 70 °C and results are presented in Figure 3.a. In this study, only the equilibrium plateau is considered, which corresponds to a saturation level $M_m=1.15\%$. The diffusion coefficient $D = 1.05 \text{ E-11 m}^2\text{s}^{-1}$ is determined by numerical optimization as presented previously. The diffusion behaviour of vinylester resin is well adjusted to the Fick's law solution given by Equation 9. Furthermore, for neat Elium™ resin coupons, the numerical fitting method of the Fick's law solution in the 1D case cannot be applied since no equilibrium plateau is reached and so no maximum moisture content value is available. Regarding this absence of a saturation plateau for Elium™ resin samples while composite ones have clearly reached equilibrium, we suggest that resin samples have a saturation level that was not reached yet during test duration. A non-Fickian model is thus set up to model the water uptake of aged Elium™ resin samples. This model is based on the assumption that two diffusion processes take place simultaneously, but with different speed rates and maximum capacities for absorbing water. The parallel dual Fick (PDF) model is generally based on the assumption that

the physical mechanism linked to the diffusion of water molecules in free volumes and the chemical mechanism where water molecules bind strongly to certain hydrophilic functional groups such as resin hydroxyls, occur simultaneously [40]. This two-stage moisture transport model has been used to interpret wet aging tests when the water uptake curves deviate from Fick's law solution[17,45,46]. In this case, two Fick's processes are assumed to occur in parallel with two different diffusion coefficients D_1 , D_2 and water concentration levels c_1 , c_2 so that the modified Fick's second law is now:

$$\frac{\partial c_1}{\partial t} + \frac{\partial c_2}{\partial t} = D_1 \frac{\partial^2 c_1}{\partial x^2} + D_2 \frac{\partial^2 c_2}{\partial x^2} \quad \text{Equation 11}$$

The analytic solution for this dual Fick equation is the sum of two solutions of Equation 9 with independent parameters. After solving, applying boundary conditions and integrating over thickness, the solution can be then written as:

$$M_t = M_{m,1} \left\{ 1 - \frac{8}{\pi^2} \sum_{n=0}^{\infty} \frac{1}{(2n+1)^2} \exp\left(\frac{-\pi^2 D_1 t (2n+1)^2}{e^2}\right) \right\} + M_{m,2} \left\{ 1 - \frac{8}{\pi^2} \sum_{n=0}^{\infty} \frac{1}{(2n+1)^2} \exp\left(\frac{-\pi^2 D_2 t (2n+1)^2}{e^2}\right) \right\} \quad \text{Equation 12}$$

where $M_{m,1}$ and $M_{m,2}$ are two saturation levels corresponding to each individual diffusion process. The sum of these contents gives the total water content at saturation M_{∞} . Using this parallel dual Fickian (PDF) model, anomalous water uptake is usually decomposed into a “fast” and “slow” processes. According to the literature, the use of this PDF model can be justified in different ways : First, the two processes correspond to a diffusion occurring in parallel in two distinct phases of the material [47]. It may be also due to a relaxation process (“bound” water diffusion) occurring in parallel with the normal Fickian diffusion (“free” water diffusion) [45,48,49]. Bao and Yee justified their use of the PDF model by the water tendency to fill the voids and cracks momentarily after water immersion, more specifically those at the surface, resulting in a fast initial uptake and then slower diffusion through the polymer matrix [18]. Figure 3.b shows the experimental data of hydrothermal aging of Elium™ resin specimens compared to the

adjusted PDF model data, with a representation of each part of the diffusion to figure out the diffusion rate difference. In the beginning of the curve, the behaviour is mostly Fickian and the water absorption is in the "free" state. However, as more water gain access to the material, the diffusion rate is slowed. This can be explained by two phenomena: As mass is gained, more water molecules are bonded to the polymer chains. This reduces the amount of molecules, which can be absorbed in classic diffusion by limiting the space in the nanopores. Secondly, the relaxation rate becomes larger than the diffusion rate and governs the rest of the absorption process [50,51]. The results of diffusion parameters identification for both resins are presented in Table 3. For vinylester resin, water uptake parameters are optimised since no degradation took place. For Elium™ resin, a considerable difference between the diffusion rates, suggesting that relaxation in the acrylic resin is a slow mechanism. If we consider the comparison of VE resin behaviour to the first stage of Elium™ resin diffusion behaviour, a good similarity is obtained.

Table 3 : Identification of water diffusion parameters into vinylester and Elium™ neat resins via data fitting

Vinylester neat resin		Elium™ 188-O neat resin			
D [m ² .s-1]	M _∞ [%]	D ₁ [m ² .s-1]	M _{m,1} [%]	D ₂ [m ² .s-1]	M _{m,2} [%]
1.05 E-11	1.15	2.30 E-11	1.49	1.38 E-14	16.04

3.3.2. Case of composites

Several specimens of different aspect ratios are immersed in deionised water at 70 °C. As shown in Figure 4 in section 3.1.2, the behaviour of these composites is non-Fickian. After reaching pseudo-equilibrium, the water content of CF / VE samples decreases gradually as if there is leaching of the material. This phenomenon was also observed by Larbi et al [39], Sobrinho et al [52], Lee et al. [53] in vinylester or other resin systems. According to Abeyshinghe et al. [54], the mechanism of weight loss can be attributed to the diffusion of residual water-soluble and volatile compounds in case of incomplete polymerization, breakdown of ester groups mainly for polyester resins hydrolysis induced by cracks and leaching. Some polyester and vinylester resins exhibit

weight loss after reaching a maximum water uptake, especially when immersed at high temperature. Leaching is generally a non-reversible thermally activated degradation mechanism, during which a loss in the chemical integrity occurs under the effect of solvent. In fact, when macromolecular chain breaks between crosslinking points, there is creation of fragments of molecular chains, which became free in the network and could diffuse towards the outside environment. The weight loss of samples during aging makes the identification of diffusion parameters more complicated. Lee et al. [53] have described the fact that the correct diffusion coefficient D cannot be obtained for a polymer which has a significant loss of weight due to leaching mechanism because this value is strongly dependent to M_m . In order to assess diffusion parameters, the same PDF model presented above is applied to the experimental water content data of CF / VE aged composites. The comparison of experimental and fitted data are presented in Figure 4.a. The weight gain can be divided into two distinct behaviours. The first is Fickian absorption behaviour with a maximum water content determined via the numerical model. It's noteworthy that the rule of mixture is perfectly applicable, taking into account the $38.7\% \pm 0.24$ of matrix volume fraction in CF / VE composites. The water content at saturation of the Fickian diffusion part is a little bit higher than the experimental data, suggesting the presence of parallel weight loss behaviour. The second curve corresponds to a mass loss linked with all previously listed phenomena and takes place in parallel with the water absorption phase. The use of PDF model to fit experimental data in this case is justified by the fact that the leaching promotes the extraction of compounds as water-soluble organic non-bound substances. Boinard et al. [55] described the leach as 'free' non-crosslinked monomer residues. Bagis and Rueggeberg found that non post-cured resins leach considerably more unreacted monomer than post-cured resins[56]. This explains the noticeable weight loss found here, as no post-cure was performed on CF/VE samples. Furthermore, the diffusion process in carbon-fibre-reinforced Elium™ 188-O composite samples also exhibits an anomaly over Fickian behaviour. The difference between the behaviour of neat Elium™ 188-O resin and CF / Elium™ samples is that the diffusion process is gradual until reaching the beginning of an equilibrium plateau after about 3600 hours of

immersion. The PDF model is used to fit experimental curves and results are presented in Figure 4.b. By analysing the beginning of the curve, it is noted that the first stage diffusion process shows a rapid increase in the water content until around 100 hours, representing the time at which the relaxation mechanisms took the lead on the Fickian water diffusion. The relatively important values of water content at saturation of the composite, compared to what they should be taking into account the rule of mixtures, the matrix volume content (33.8%) and the estimated water content at saturation of neat Elium™ resin (16.04 %) suggest that water diffuses not only in bulk resin, but also in free volume and by capillarity in the fibre/matrix interstices as presented by SEM micrographs in §3.4. In addition, the maximum water content of the first stage of the composite is different from expected value taking into account maximum water content of first stage of neat Elium™ resin (1.49 %) and the matrix volume content of studied composite plates. This can be explained by already presented non-Fickian behaviour of neat Elium™ resin, and, when immersed, composites absorb water by classical Fickian diffusion in bulk resin and by surface defects. After the first stage, total water content continues then to increase gradually and slowly compared to the first part ($D_1 > D_2$) until reaching an equilibrium state. Identified parameters for CF / VE and CF / Elium™ composites are presented in Table 4. Comparing the first part of PDF identified parameters (D_1 and $M_{m,1}$) of each composite, diffusion coefficient of the first stage is three times higher in CF / Elium™ than in CF / VE composites. In addition, first saturation content is significantly higher for acrylic composites.

Table 4 : Identification of water diffusion parameters into CF / VE and CF / Elium™ composites via data fitting

Diffusion parameters	CF / VE	CF / Elium™
	180×180×2.5	180×180×2.5
D_1 [m ² .s ⁻¹]	2.91 E-12	9.62 E-12
$M_{m,1}$ [%]	0.45	1.68
D_2 [m ² .s ⁻¹]	1.35 E-13	1.52 E-13
$M_{m,2}$ [%]	-0.27	5.24

3.4. Scanning electron microscope SEM

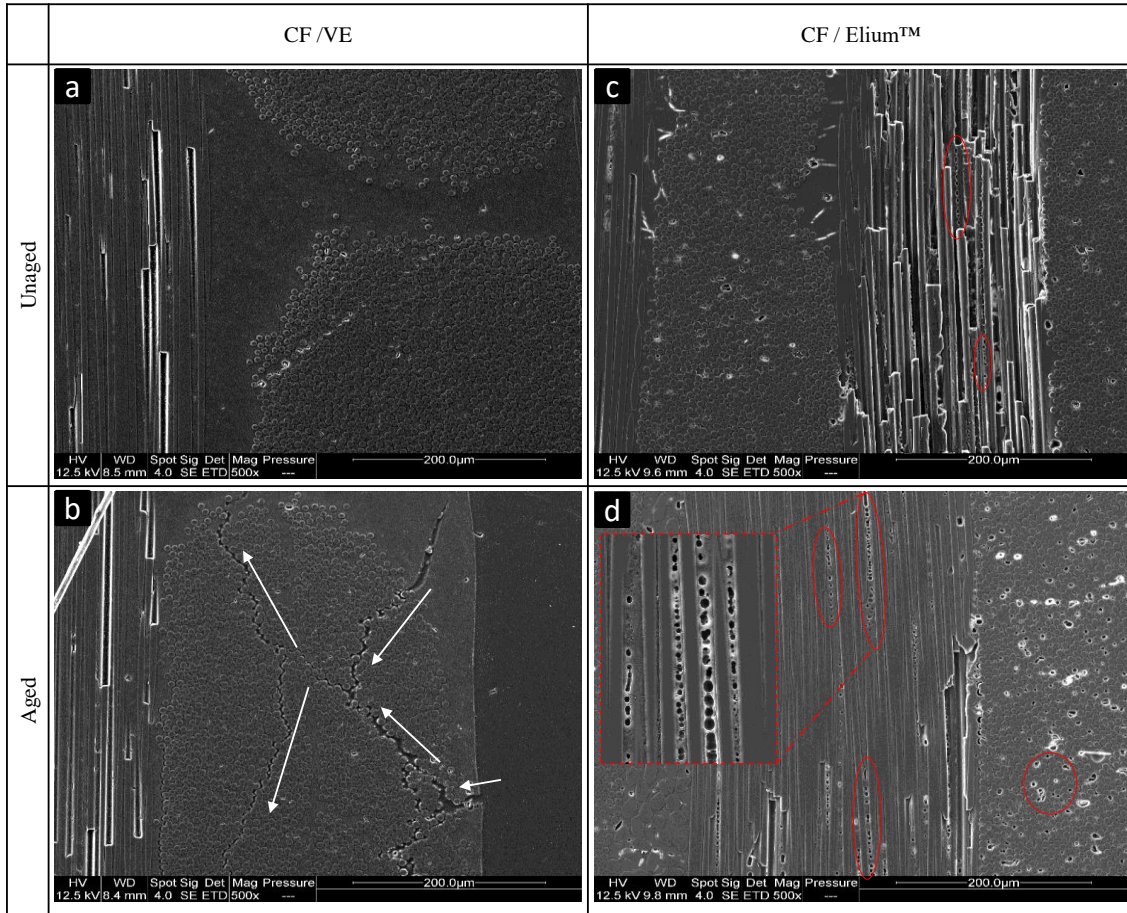


Figure 7 : SEM graphs of the cross section surface of both materials for unaged (a and c) and aged (b and d) specimens

SEM observations were conducted on samples before aging and after 5000h of water immersion. For CF / VE composites (Figure 7.a and Figure 7.b), water enters from outer lamina defects and starts to propagate progressively at the fibre/matrix interface causing delamination and hydrolysis of the side groups and leaching of unreacted monomer species. In addition, water absorption into the matrix and thus swelling generates high stress levels at the fibre / matrix interface, which can be spotted by the debonding at the interface. The same phenomena were reported by Hodzic et al. [57]. In images a and c, unaged specimens of CF / VE and CF / Elium™ are presented, respectively. Unlike vinylester composites, which presents good wetting of the fibres at unaged state, Elium™ composites presents poor fibre/matrix interface quality marked by the presence of

voids. Those structural defects seem to be caused by the poor compatibility between the fibre and matrix, as the fabric have a compatibility with epoxy and epoxy modified thermoset resin and not with acrylic resins. According to a recent study of Hendlmeier et al. [58], the epoxy sizing is soluble in MMA monomer and could be removed from fibre surface before complete polymerisation. The voids at fibre/matrix walls can also partly explain the important amounts of water absorbed by CF / Elium™ composites when immersed in deionised water at relatively high temperature (70 °C). However, the results should be considered with great caution due to the influence of the specimen preparation method (composite cutting, grinding and polishing) and test conditions (low vacuum and high electron beam intensity) on interface quality [59]. The images and observations at unaged state are in fact useful to inspect the defect and damage progress in both materials when submitted to hydrothermal aging. In Figure 7.d, one can remark the effect of water ingress on the microstructure. For aged CF / Elium™ composites, a closer view of voids showed matrix damage and formation of pot holes as seen by Sharma et al. in epoxy matrix [60]. A considerable growth of voids and defects may explain the large duration before reaching saturation at high water contents. So, the quality of the fibre / matrix cohesion at the interface is very important if moisture diffuse along this interface.

3.5. Influence of water absorption on mechanical properties

3.5.1. Tensile tests

Young modulus, shear modulus and tensile strength were determined by uniaxial tensile test on both materials. The tensile tests are performed in longitudinal (0°/90°) and off-axis (+45°/-45°) direction until breaking. Modulus was evaluated in the strain interval of 0.05 – 0.25% using linear regression. For each set of samples, a minimum of 4 specimens are tested. Figure 8 shows the stress-strain curves under uniaxial tensile test of 0°/90° CF / Elium™ and CF / VE materials at the reference and final aged states (see Figure 1). In each curve, the transverse ϵ_{xx} and longitudinal ϵ_{yy} strains are presented. For both composites at unaged and aged states, the in-plane strain ϵ_{xy} results confirms the overlay of reference frames corresponding to the recording camera, loading

and orthotropic of composite reinforcement. The balanced biaxial fabric used for the samples preparation explains the high transverse modulus compared to longitudinal one, and so the low poisson's ratio for each material in both aged and unaged states. In all cases, the tensile curves are linear and confirm the rigid behaviour of studied composites.

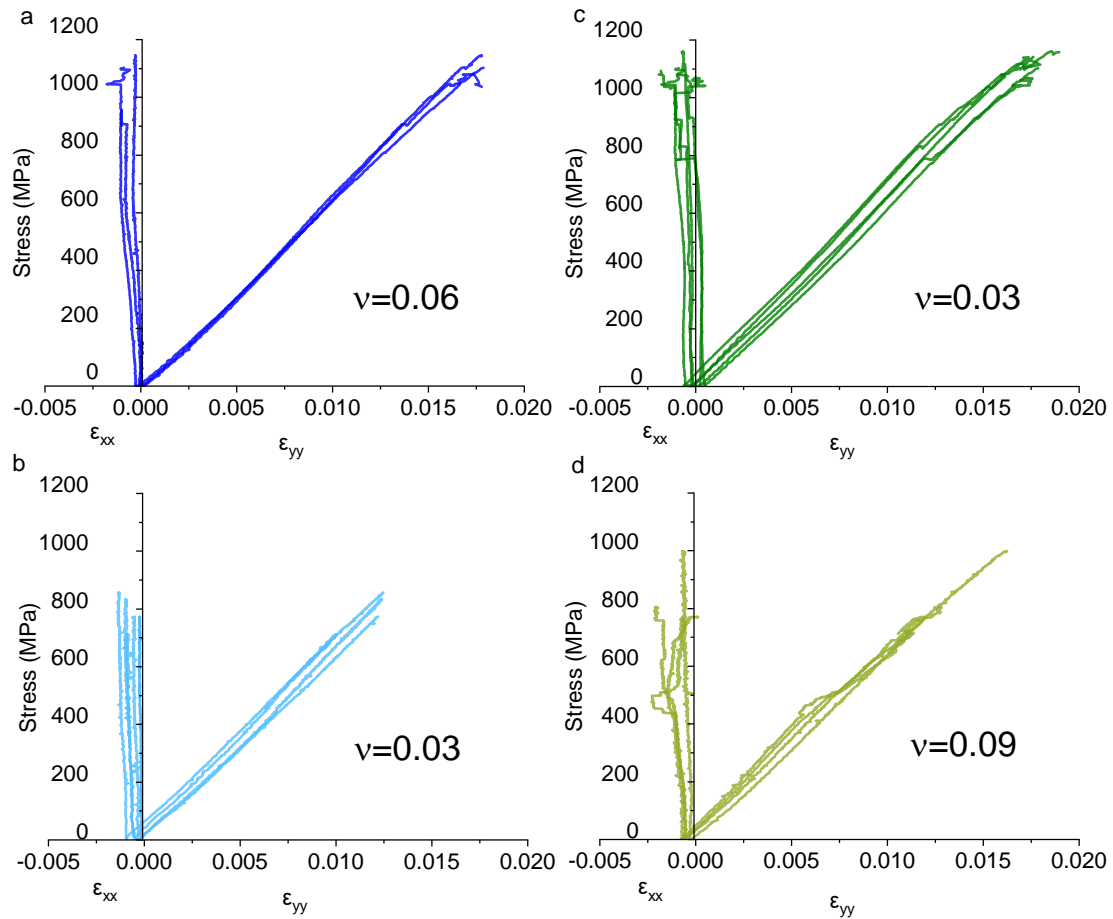


Figure 8 : Tensile stress-strain curves of $0^{\circ}/90^{\circ}$ specimens : (a) unaged CF / VE specimens, (b) aged CF / VE specimens, (c) unaged CF / Elium™ specimens and (d) aged CF / Elium™ specimens

The mean values of tensile modulus and ultimate shear strength in the unaged and aged situation for both composite materials are presented in Figure 9. A small decrease of around 6% in the tensile modulus of CF / Elium™ specimens between unaged and aged states, while a nearly similar modulus is found for CF / VE material. For the ultimate tensile stress, a similar degradation level of about 10% is found for both materials at different states. This good resistance

after around 6 months of immersion in deionised water at 70 °C is related to the good stability of carbon fibres in such conditions and the fact that the tensile load applied on the specimens on the longitudinal directions involves principally the fibres.

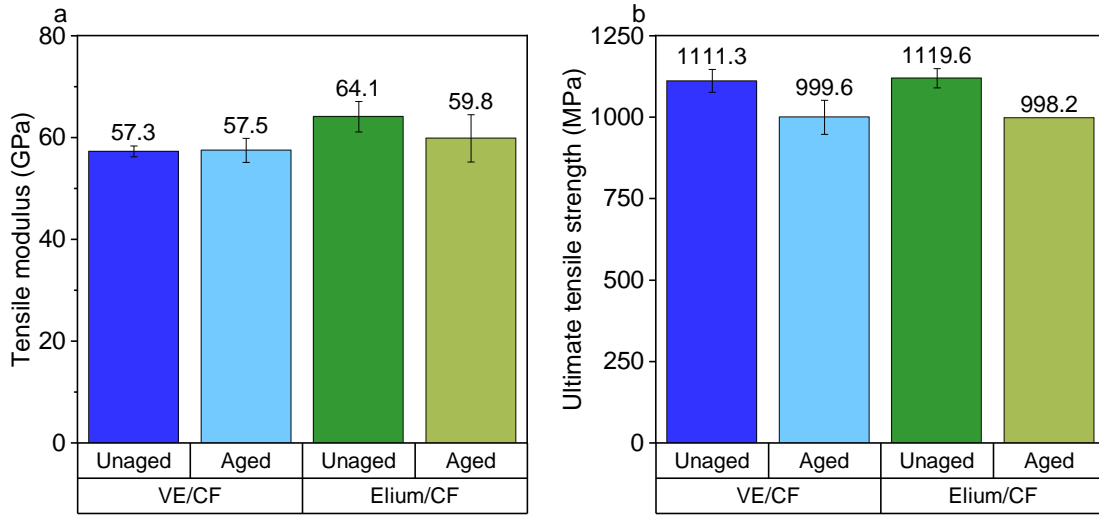


Figure 9 : Tensile modulus (a) and ultimate tensile strength (b) properties obtained by longitudinal tensile test for both aged and unaged CF / Elium™ and CF / Elium™ CF / VE samples

To evaluate the shear modulus, and to assess the degradation levels of the composite materials after aging, off-axis tensile tests were performed. They consist on monotonic tensile tests on samples whose fiber direction is +45°/-45°. The stress-strain curves related to this off-axis test are presented in Figure 10. Transverse ϵ_{xx} and longitudinal ϵ_{yy} strains are monitored for both materials in both unaged and aged states. For CF / Elium™ composites under off-axis tensile test in aged state, the ultimate stress level at breaking is reduced by around 17% (Figure 11.b). In this type of tests, the matrix behaviour is more important since the load is not in the fibre directions. The maximum strain at breaking is also largely altered by aging, which proves the decrease in the ductility of the material. One also can remark that the maximum elastic stresses and strains have not changed during aging and it is only the plastic part, which is significantly reduced. For CF / VE composite, the ultimate stress level is also reduced by around 27% (Figure 11.b). With respect to CF / VE composite, a significant loss in ultimate stress is observed while aging the samples,

but the strain level at maximum stress is not impacted. Unlike results of CF / Elium™ composites, the maximum elastic stress level is much lower after aging, while elastic strain is not impacted.

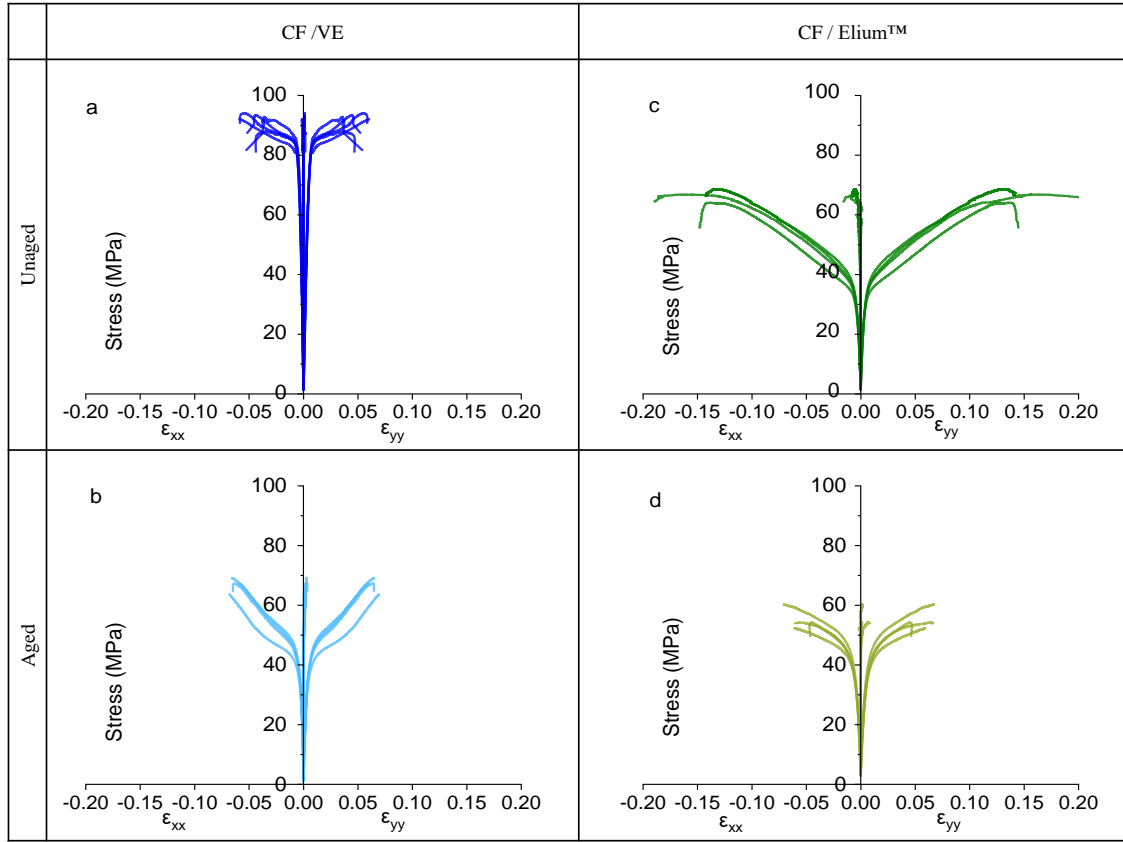


Figure 10 : Tensile stress-strain curves of +45°/-45° (a) unaged CF / VE specimens, (b) aged CF / VE specimens, (c) unaged CF / Elium™ specimens and (d) aged CF / Elium™ specimens

The shear modulus G is calculated from both previous test results for each material using the following equation:

$$\frac{1}{G} = \frac{4}{E_{45}} - \frac{1}{E_L} - \frac{1}{E_T} + 2 \frac{\nu_{LT}}{E_L} \quad \text{Equation 13}$$

E_L , E_T and ν_{LT} are tensile moduli and Poisson's ratio obtained from tensile tests in longitudinal and transverse directions, E_{45} is the apparent modulus measured from off-axis test. In this case, $E_L = E_T$ because the biaxial fabric used is balanced. Figure 11.a shows the variation of the longitudinal shear modulus before and after aging. For dry specimens, the shear modulus of CF / Elium™ samples is around the half of the shear modulus of CF / VE. The water absorption induces a drop in the shear modulus values after saturation, and this change is more significant for CF /

VE samples (47 % compared to just 8% for CF / Elium™ composites). This leads to suggest that, for VE resin, irreversible degradations took place during aging, and they are behind the drop in shear modulus and ultimate shear strength for aged CF / VE material.

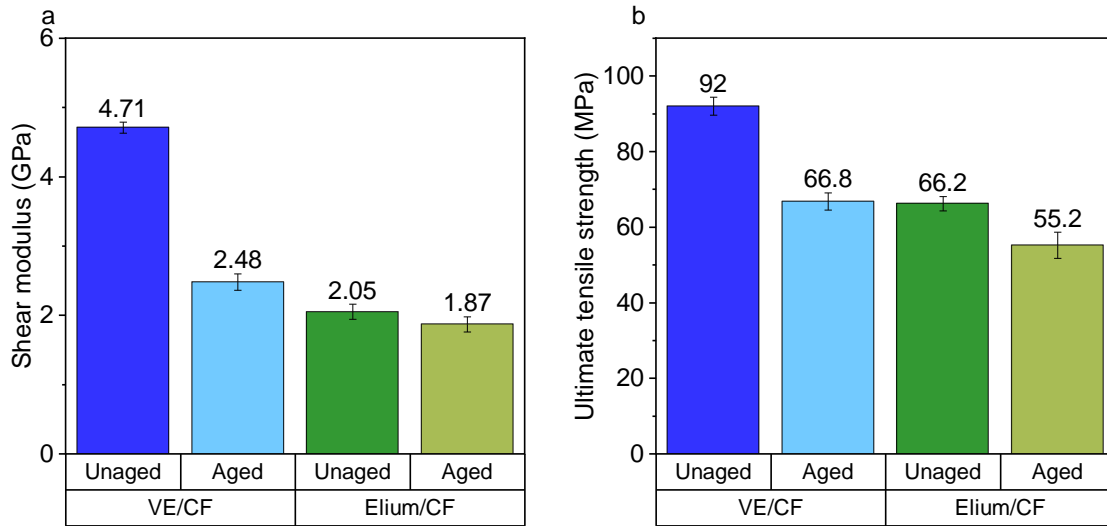


Figure 11 : Shear modulus (a) and ultimate tensile strength (b) properties obtained by off-axis tensile test for both aged and unaged CF / VE and CF / Elium™ specimens

3.5.2. Interlaminar shear strength ILSS

Interlaminar shear strength (ILSS) is predominately governed by interfacial bonding between reinforcing fibres and matrix at interphase and interply regions [61]. The strength is determined by the first apparent discontinuity and drop in the load-displacement curve. Recent standards have shown increased insistence on the accepted failure modes, with only interlaminar failure being accepted. Standard force vs displacement curves of ILSS test are reported in Figure 12. When specimens of both materials were tested, just few interlaminar failures were observed, and the majority exhibited unacceptable failure modes like tension failure or plastic deformation. Tests on unaged CF / Elium™ 5 mm thick specimens show significant dispersion of the results that is mainly related to the void volume fraction, which is around 4.8 %, compared to 2.1 % for CF / VE 5 mm thick samples. For the latter, the average maximum force passes from 1838.5 N at the unaged state to 1139.9 N after aging, which represents 38% of loss. For CF / Elium™ samples, the standard force decrease is around 43%. Short beam strengths, calculated from Equation 6, are

presented in Figure 13. As the calculation depends on the standard force values and samples dimensions, the same trend is observed. A quite significant loss in strength caused by water ingress into the thick material, which strengthen the hypothesis that fibre/matrix interface is largely dependent on the water content in the material. Those ILSS results should be taken with precautions to quantitatively compare composite interlaminar shear strength between studied composites. This prudence is raised by the relatively low results found in this study and the absence of comparable results of Elium™ 188-O composites.

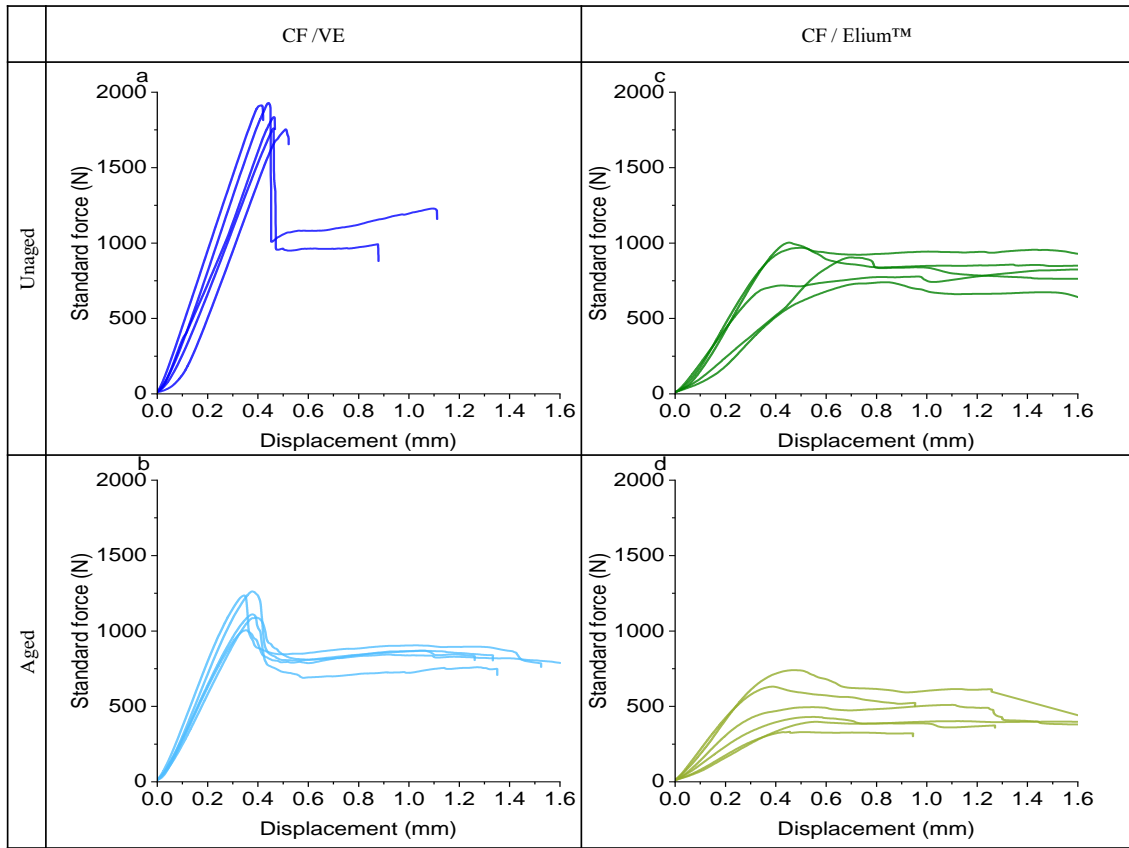


Figure 12 : ILSS force-deformation curves of (a) unaged CF / VE specimens, (b) aged CF / VE specimens, (c) unaged CF / Elium™ specimens and (d) aged CF / Elium™ specimens

In the literature, few authors were interested to ILSS of Elium™ based composites compared to thermoset counterparts and a significant dispersion of their results is noted due to different test method and standards used (ASTM D2344, ISO 14130, NF EN 6585, etc.). Test apparatus, recommended specimen dimensions and test speed rate are different in each case. This dispersion

of results can also be related to the use of different fabric (UD, woven, multiaxial NCF ...) and fibre sizing types. Davies and Arhant noted that Elium™ 180 / triaxial carbon fibre 3.7 mm thick ILSS specimen failed in compression [26]. Nash et al. reported a relatively high ILSS value for quasi-UD glass fibre reinforced Elium™ 150 (around 57 MPa). After aging, a loss of nearly half the reference value is found [11].

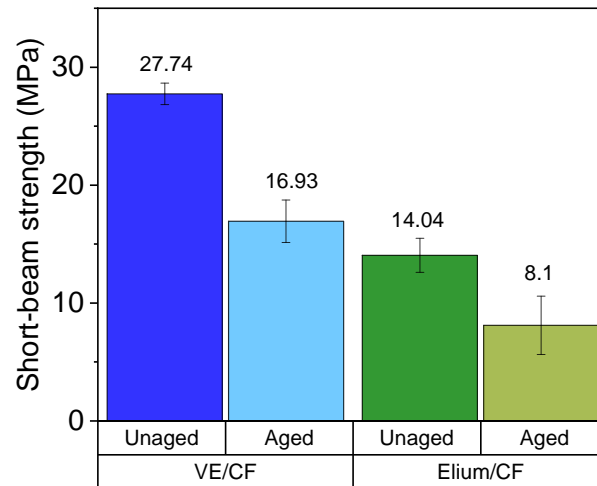


Figure 13 : Short beam strength properties obtained by ILSS test for both aged and unaged CF / Elium™ and CF / VE specimens

4. Conclusion

The aim of this study was to study the behaviour of a carbon fibre reinforced Elium™ acrylic thermoplastic composite compared to a carbon fibre reinforced vinylester composite during hydrothermal aging at 70 °C. In the one hand, for the vinylester neat resin, the observed diffusion behaviour is Fickian and diffusion parameters are determined. On the other hand, the Elium™ resin behaves differently when immersed in deionised water at 70 °C. The water content increases gradually without reaching saturation. This phenomenon could be related to the hydrolysis of the side groups of the resin and thus relaxation caused by high aging temperature leading to the increase of free volume in the bulk resin. Applying a numerical fitting, a dual Fickian model is suggested regarding the relaxation and/or chemical degradation. In the case of CF / VE composites, the behaviour appears to be Fickian until the onset of degradation caused by leaching,

resulting in significant loss of weight. A numerical model is proposed to decompose this competitive behaviour into absorption behaviour and another related to desorption. CF / Elium™ composites also exhibit pseudo-Fickian behaviour, where the absorption mechanism is retarded by the relaxation of the polymer. The equilibrium reached at the end of aging makes it possible to model the phenomenon while considering polymer relaxation. The use of the same Parallel Dual Fickian model to VE and acrylic reinforced composites is justified by the need to compare diffusion kinetics of both materials. Comparison of the first stage of applied model leads to conclude on the similarity of the water uptake mechanisms. The onset of deviation from Fick's law is related to thermally activated degradations. Mechanical properties show good agreement and similarities between both materials. For longitudinal tensile properties, not significant changes are reported, due to the main action of carbon fibre. However, off-axis tensile properties as well as interlaminar shear strength results present more dependency to the aged matrix behaviour, resulting in important loss of properties, more specifically for CF/VE compared to CF/Elium composite. Then, the changes in the microstructure are evaluated by SEM, where clear fibre/matrix debonding was observed. Finally, the reversibility of aging effects on both resins and composites shows that all samples undergo irreversible changes, more particularly for vinyl ester reinforced composites which are related to chemical degradation during immersion in high temperature water. A perspective of this work is to investigate the effect of other aging conditions and environments on the substitution material response in order to produce a benchmark for later industrial application.

5. Acknowledgment

Authors would like to acknowledge the financial support from Occitanie region in France and REV inside, France as project partner. The authors would like to thank Pierre GERARD from ARKEMA for the supply of Elium™ resin.

Declarations

Declaration of interests

The authors declare that they have no known competing financial interests or personal relationships that could have appeared to influence the work reported in this paper.

Data availability statement

The raw/processed data required to reproduce these findings cannot be shared at this time as the data also forms part of an ongoing study.

Authors' contributions

Haithem Bel Haj Frej: Conceptualization, Methodology, Software, Formal analysis, Investigation, Writing - Original Draft, Visualization

Romain Léger: Conceptualization, Methodology, Validation, Resources, Writing - Review & Editing, Supervision

Didier Perrin: Conceptualization, Methodology, Validation, Resources, Writing - Review & Editing, Supervision

Patrick Ienny: Conceptualization, Methodology, Validation, Resources, Writing - Review & Editing, Supervision, Project administration

6. References

- [1] Swan D, Gerard P. Novel reactively polymerized liquid thermoplastic resins process like thermosets but offer post-mold, thermoformability, weldability, recyclability. 2014.
- [2] Obande W, Ray D, Ó Brádaigh CM. Viscoelastic and drop-weight impact properties of an acrylic-matrix composite and a conventional thermoset composite – A comparative study. Mater Lett 2019;238:38–41. doi:10.1016/j.matlet.2018.11.137.
- [3] Bhudolia SK, Perrotey P, Joshi SC. Optimizing polymer infusion process for thin ply textile composites with novel matrix system. Materials (Basel) 2017;10. doi:10.3390/ma10030293.
- [4] Obande W, Mamalis D, Ray D, Yang L, Ó Brádaigh CM. Mechanical and

- thermomechanical characterisation of vacuum-infused thermoplastic- and thermoset-based composites. *Mater Des* 2019;175:107828. doi:10.1016/j.matdes.2019.107828.
- [5] Murray RE, Swan D, Snowberg D, Berry D, Beach R, Rooney S. Manufacturing a 9-Meter Thermoplastic Composite Wind Turbine Blade. 32nd Tech Conf Am Soc Compos 2017:29–43.
- [6] Hassen AA, Springfield R, Lindahl J, Post B, Love L, Duty C, et al. The Durability of Large-Scale Additive Manufacturing Composite Molds. CAMX – Compos. Adv. Mater. Expo, Anaheim: 2016.
- [7] Boufaida Z, Farge L, André S, Meshaka Y. Influence of the fiber/matrix strength on the mechanical properties of a glass fiber/thermoplastic-matrix plain weave fabric composite. *Compos Part A Appl Sci Manuf* 2015;75:28–38. doi:10.1016/j.compositesa.2015.04.012.
- [8] Raponi O de A, Barbosa LCM, de Souza BR, Ancelotti Junior AC. Study of the influence of initiator content in the polymerization reaction of a thermoplastic liquid resin for advanced composite manufacturing. *Adv Polym Technol* 2018;37:3579–87. doi:10.1002/adv.22142.
- [9] Kinvi-Dossou G, Matadi Boumbimba R, Bonfoh N, Garzon-Hernandez S, Garcia-Gonzalez D, Gerard P, et al. Innovative acrylic thermoplastic composites versus conventional composites: Improving the impact performances. *Compos Struct* 2019;217:1–13. doi:10.1016/j.compstruct.2019.02.090.
- [10] Bhudolia SK, Joshi SC, Bert A, Yi Di B, Makam R, Gohel G. Flexural characteristics of novel carbon methylmethacrylate composites. *Compos Commun* 2019;13:129–33. doi:10.1016/j.coco.2019.04.007.
- [11] Nash NH, Portela A, Bachour-Sirerol CI, Manolakis I, Comer AJ. Effect of environmental conditioning on the properties of thermosetting- and thermoplastic-matrix composite materials by resin infusion for marine applications. *Compos Part B Eng* 2019;177:107271. doi:10.1016/j.compositesb.2019.107271.

- [12] Choqueuse D, Davies P. Ageing of composites in underwater applications. *Ageing Compos.*, Elsevier; 2008, p. 467–98. doi:10.1533/9781845694937.3.467.
- [13] Summerscales J. Materials selection for marine composites. In: Pemberton R, Summerscales J, Graham-Jones J, editors. *Mar. Compos. Des. Perform.*, Elsevier, 2019; 2019, p. 3–30. doi:10.1016/B978-0-08-102264-1.00001-7.
- [14] Mortaigne B. Vieillissement des composites-Mécanismes et méthodologie d'étude. *Téchniques de l'ingénieur* 2005;AM5320 V1.
- [15] Crank J. *The mathematics of diffusion*. Clarendon Press; 1979.
- [16] Pemberton R, Summerscales J, Graham-Jones J. *Marine Composites : Design and Performance*. Woodhead Publishing series in Composites Science and Engineering; 2019.
- [17] Bao L-R, Yee AF. Moisture diffusion and hygrothermal aging in bismaleimide matrix carbon fiber composites: part II—woven and hybrid composites. *Compos Sci Technol* 2002;62:2111–9. doi:10.1016/S0266-3538(02)00162-8.
- [18] Bao LR, Yee AF. Moisture diffusion and hygrothermal aging in bismaleimide matrix carbon fiber composites: Part II-woven and hybrid composites. *Compos Sci Technol* 2002;62:2111–9. doi:10.1016/S0266-3538(02)00162-8.
- [19] Roy S, Xu WX, Park SJ, Liechti KM. Anomalous Moisture Diffusion in Viscoelastic Polymers: Modeling and Testing. *J Appl Mech* 2000;67:391. doi:10.1115/1.1304912.
- [20] Chen X, Zhao S, Zhai L. Moisture Absorption and Diffusion Characterization of Molding Compound. *J Electron Packag* 2005;127:460. doi:10.1115/1.2065707.
- [21] Y. Weitsman, Cai L-W. *Non-Fickian Moisture Diffusion in Polymeric Composites*. Virginia: 1992.
- [22] Carter HG, Kibler KG. Langmuir-Type Model for Anomalous Moisture Diffusion In Composite Resins. *J Compos Mater* 1978;12:118–31. doi:10.1177/002199837801200201.
- [23] El Yagoubi J, Lubineau G, Roger F, Verdu J. A fully coupled diffusion-reaction scheme

- for moisture sorption–desorption in an anhydride-cured epoxy resin. *Polymer (Guildf)* 2012;53:5582–95. doi:10.1016/j.polymer.2012.09.037.
- [24] Leger R, Roy A, Grandidier JC. Non-classical water diffusion in an industrial adhesive. *Int J Adhes Adhes* 2010;30:744–53. doi:10.1016/j.ijadhadh.2010.07.008.
- [25] Davies P. Environmental degradation of composites for marine structures: new materials and new applications. *Philos Trans R Soc A Math Phys Eng Sci* 2016;374:20150272. doi:10.1098/rsta.2015.0272.
- [26] Davies P, Arhant M. Fatigue Behaviour of Acrylic Matrix Composites: Influence of Seawater. *Appl Compos Mater* 2019;26:507–18. doi:10.1007/s10443-018-9713-1.
- [27] Davies P, Le Gac P-Y, Le Gall M. Influence of Sea Water Aging on the Mechanical Behaviour of Acrylic Matrix Composites. *Appl Compos Mater* 2017;24:97–111. doi:10.1007/s10443-016-9516-1.
- [28] Arhant M, Davies P. Thermoplastic matrix composites for marine applications. In: Pemberton R, Summerscales J, Graham-Jones J, editors. *Mar. Compos. Des. Perform.*, Elsevier, 2019; 2019, p. 31–53. doi:10.1016/B978-0-08-102264-1.00002-9.
- [29] Arkema. Elium 188: Technical datasheet. 2015.
- [30] Springer GS, Loos AC. Moisture Absorption of Graphite-Epoxy Composites Immersed in Liquids and in Humid Air. *J Compos Mater* 1979;13:131–47.
- [31] Deroiné M, Le Duigou A, Corre Y, Le Gac P-Y, Davies P, César G, et al. Accelerated ageing of polylactide in aqueous environments: Comparative study between distilled water and seawater. *Polym Degrad Stab* 2014;108:319–29. doi:10.1016/j.polymdegradstab.2014.01.020.
- [32] ASTM D 5229/D 5229M – 92. Standard Test Method for Moisture Absorption Properties and Equilibrium Conditioning of Polymer Matrix Composite Materials 2004.
- [33] Christmann A, Ienny P, Quantin JC, Caro-Bretelle AS, Lopez-Cuesta JM. Mechanical behaviour at large strain of polycarbonate nanocomposites during uniaxial tensile test. *Polymer (Guildf)* 2011;52:4033–44. doi:10.1016/j.polymer.2011.06.056.

- [34] Silva MAG, da Fonseca BS, Biscaia H. On estimates of durability of FRP based on accelerated tests. *Compos Struct* 2014;116:377–87.
doi:10.1016/j.compstruct.2014.05.022.
- [35] Weitsman YJ. *Fluid Effects in Polymers and Polymeric Composites*. Boston, MA: Springer US; 2012. doi:10.1007/978-1-4614-1059-1.
- [36] Tham WL, Chow WS, Ishak ZAM. Simulated body fluid and water absorption effects on poly(methyl methacrylate)/hydroxyapatite denture base composites. *Express Polym Lett* 2010;4:517–28. doi:10.3144/expresspolymlett.2010.66.
- [37] Mangin R. *Influence du vieillissement sur le comportement au feu de formulations hétérophasées ignifugées*. Univerilté de Lorraine, 2018.
- [38] Kootsookos A, Mouritz AP. Seawater durability of glass- and carbon-polymer composites. *Compos Sci Technol* 2004;64:1503–11.
doi:10.1016/j.compscitech.2003.10.019.
- [39] Larbi S, Bensaada R, Bilek A, Djebali S. Hygrothermal ageing effect on mechanical properties of FRP laminates. *AIP Conf. Proc.* 1653, vol. 020066, 2015, p. 020066.
doi:10.1063/1.4914257.
- [40] Zhou J, Lucas JP. The effects of a water environment on anomalous absorption behavior in graphite/epoxy composites. *Compos Sci Technol* 1995;53:57–64. doi:10.1016/0266-3538(94)00078-6.
- [41] Yao J, Ziegmann G. Water absorption behavior and its influence on properties of GRP pipe. *J Compos Mater* 2007;41:993–1008. doi:10.1177/0021998306067265.
- [42] Silva LV da, Silva FW da, Tarpani JR, Forte MM de C, Amico SC. Ageing effect on the tensile behavior of pultruded CFRP rods. *Mater Des* 2016;110:245–54.
doi:10.1016/j.matdes.2016.07.139.
- [43] Arhant M, Le Gac PY, Le Gall M, Burtin C, Briançon C, Davies P. Effect of sea water and humidity on the tensile and compressive properties of carbon-polyamide 6 laminates. *Compos Part A Appl Sci Manuf* 2016;91:250–61.

- doi:10.1016/j.compositesa.2016.10.012.
- [44] Pritchard G. Reinforced plastics durability. Woodhead P. CRC Press LLC; 1999.
doi:10.1533/9781845694876.186.
- [45] Placette MD, Fan X, Jie-Hua Zhao, Edwards D. A dual stage model of anomalous moisture diffusion and desorption in epoxy mold compounds. EuroSimE 12, IEEE; 2011. doi:10.1109/ESIME.2011.5765824.
- [46] Cocaud J, Céline A, Fréour S, Jacquemin F. Vers une méthodologie d'identification des paramètres de diffusion d'eau dans les polymères et composites. Journées Natl. sur les Compos., Champs-Sur-Marne, France: 2017.
- [47] Ibrahim G. Comportement hygromécanique de tubes composites obtenus par enroulement filamentaire en immersion et soumis à différentes températures. 2017.
- [48] De Parscau Du Plessix B, Jacquemin F, Lefébure P, Le Corre S. Characterization and modeling of the polymerization-dependent moisture absorption behavior of an epoxy-carbon fiber-reinforced composite material. J Compos Mater 2016;50:2495–505.
doi:10.1177/0021998315606510.
- [49] Wong KJ. Moisture absorption characteristics and effects on mechanical behaviour of carbon/epoxy composite: application to bonded patch repairs of composite structures. Univ Bourgogne 2013;225. doi:10.1109/IVMSPW.2013.6611889.
- [50] Shirangi MH. Moisture Sensitivity of Plastic Packages of IC Devices. Moisture Sensit Plast Packag IC Devices 2010. doi:10.1007/978-1-4419-5719-1.
- [51] Loh WK, Crocombe AD, Wahab MMA, Ashcroft IA. Modelling anomalous moisture uptake, swelling and thermal characteristics of a rubber toughened epoxy adhesive. Int J Adhes Adhes 2005;25:1–12. doi:10.1016/j.ijadhadh.2004.02.002.
- [52] Sobrinho LL, Ferreira M, Bastian FL. The Effects of Water Absorption on an Ester Vinyl Resin System. Mater Res J Mater 2009;12:353–61. doi:10.1590/S1516-14392009000300017.
- [53] Lee SB, Rockett T, Hoffman R. Interactions of water with unsaturated polyester, vinyl

- ester and acrylic resins. *Polymer (Guildf)* 1992;33:3691–3697.
- [54] Abeysinghe HP, Edwards W, Pritchard G, Swampillai GJ. Degradation of crosslinked resins in water and electrolyte solutions. *Polymer (Guildf)* 1982;23:1785–90.
doi:10.1016/0032-3861(82)90123-9.
- [55] Boinard E, Pethrick RA, Dalzel-Job J, Macfarlane CJ. Influence of resin chemistry on water uptake and environmental ageing in glass fibre reinforced composites-polyester and vinyl ester laminates. *J Mater Sci* 2000;35:1931–7. doi:10.1023/A:1004766418966.
- [56] Bagis YH, Rueggeberg FA. The effect of post-cure heating on residual, unreacted monomer in a commercial resin composite. *Dent Mater* 2000;16:244–7.
doi:10.1016/S0109-5641(00)00006-3.
- [57] Hodzic A, Kim JK, Lowe AE, Stachurski ZH. The effects of water aging on the interphase region and interlaminar fracture toughness in polymer-glass composites. *Compos Sci Technol* 2004;64:2185–95. doi:10.1016/j.compscitech.2004.03.011.
- [58] Hendlmeier A, Marinovic LI, Al-Assafi S, Stojcevski F, Henderson LC. Sizing effects on the interfacial shear strength of a carbon fibre reinforced two-component thermoplastic polymer. *Compos Part A Appl Sci Manuf* 2019;127:105622.
doi:10.1016/j.compositesa.2019.105622.
- [59] Berges M, Léger R, Placet V, Person V, Corn S, Gabrion X, et al. Influence of moisture uptake on the static, cyclic and dynamic behaviour of unidirectional flax fibre-reinforced epoxy laminates. *Compos Part A Appl Sci Manuf* 2016;88:165–77.
doi:10.1016/j.compositesa.2016.05.029.
- [60] Sharma B, Chhibber R, Mehta R. Seawater ageing of glass fiber reinforced epoxy nanocomposites based on silylated clays. *Polym Degrad Stab* 2018;147:103–14.
doi:10.1016/j.polymdegradstab.2017.11.017.
- [61] Chamis CC. *Mechanics of Load Transfer At the Fiber - Matrix Interface*. 1972.
doi:NASA TN D-6588.